Phonons in icosahedral and cubic Al-Li-Cu

A. I. Goldman and C. Stassis
Ames Laboratory and Department of Physics and Astronomy, Iowa State University, Ames, Iowa 50011

M. de Boissieu, R. Currat, and C. Janot
Institut Laue-Langevin, 156X, 38042 Grenoble CEDEX, France

R. Bellissent and H. Moudden
Laboratoire Léon Brillouin, Centre d'Études Nucléares Saclay, 91191 Gif-sur-Yvette CEDEX, France

F. W. Gayle
Metallurgy Division, National Institute of Standards and Technology, Gaithersburg, Maryland 20899
(Received 22 August 1991)

We describe the results of inelastic-neutron-scattering measurements on single grains of icosahedral Al-Li-Cu and the related cubic R phase. Measurements along the high-symmetry twofold, threefold, and fivefold axes of the icosahedral phase clearly show the existence of well-defined propagating modes, with isotropic dispersion, near strong Bragg peaks. The spectral weight of the acoustic phonons scale linearly with the integrated intensity of the associated zone centers. In several cases we are able to identify "quasi"-Brillouin-zones, with stationary points at the "special" high-symmetry points of a simple icosahedral lattice. While the phonon dispersion for transverse and longitudinal acoustic modes along the twofold axis of the cubic R phase is quite similar to that found for the icosahedral phase, differences are found in the higher-energy modes; the behavior of the higher-energy modes of the icosahedral phase is consistent with an enhanced degree of spatial localization for these excitations.

I. INTRODUCTION

During the past five years, there have been extensive investigations into the structure of quasiperiodic alloys.[1] While studies of the dynamical properties have lagged, there has been a recent surge of interest in both theoretical and experimental determinations of the electronic and vibrational spectra of these materials. The small grain size of most icosahedral phases has limited neutron-scattering studies to measurements of the vibrational density of states (VDOS) for powder samples.[2–4] Inelastic-neutron-scattering measurements of phonons in icosahedral Al-Li-Cu (Ref. 5) and Al-Cu-Fe (Ref. 6) are now possible because of the availability of relatively large single grains of these stable phases.

The details of elementary excitations in quasicrystals are expected to differ from those found for periodic crystals. First, the absence of elastic anisotropy is expected for icosahedral alloys, since the symmetry of the icosahedral point group ($m\bar{3}\bar{5}$) is higher than cubic. Invariance of the cubic elastic constants under rotations by $2\pi/5$ about a fivefold axis leads to the isotropic relation $2c_{44}=c_{11}-c_{12}$.[7] Second, differences arise from the fundamental incommensurability of quasiperiodic structures. One consequence of this is that the concept of Brillouin zones in the reciprocal lattice is ill defined. Reciprocal space is, in principle, densely filled with Bragg peaks, although most of these peaks have negligible intensity.

Incommensurability leads to the existence of additional modes, termed "phasons,"[8–10] which are analogous to the excitations observed in other incommensurate systems such as mercury chain compounds.[11] Unlike the propagating phason modes in these systems, however, phason modes in icosahedral quasicrystals are predicted to be either diffusive or pinned.[12] Indeed, in many icosahedral alloys, such as Al-Mn and Al-Li-Cu, there is abundant evidence of "frozen-in" anisotropic phason strain.[13] This results in noticeable x-ray-powder-diffraction peak broadening accompanied by small shifts in positions or distortions in shapes of diffraction spots.[14,15] It is also believed that this form of disorder is responsible for the enhanced density of tunneling states observed for icosahedral Al-Li-Cu.[16]

The principal difficulty encountered in theoretical calculations of the dynamical response of quasicrystals is the absence of periodicity. This means that one cannot choose a fundamental structural block of atoms in three dimensions, such as a unit cell, which stacks regularly to form the crystal. Therefore, even if one could specify the interactions between an atom at some specific site on a quasilattice and its neighbors, this information cannot be used, in a straightforward manner, to specify the potential at some other site in the structure. Consequently, for N atoms in the structure, the N coupled equations of motion that govern the dynamics of the quasicrystal cannot be reduced in number.

Studies of electronic states and vibrational modes of a system with quasiperiodic potentials have been primarily concerned with calculations of the electronic and vibrational density of states (DOS) and the characteristics of wave functions in a quasiperiodic potential.[17–24] All of these calculations have been done for one- or two-

dimensional models without atomic decoration. For the case of the one-dimensional Fibonacci sequence (Fig. 1), it is now generally accepted that the DOS exhibits a dense set of gaps arranged in a self-similar hierarchical manner. The wave functions are characterized as "critical," neither extended nor exponentially localized. Experimental neutron-scattering measurements, however, have not shown evidence of a proliferation of gaps in the vibrational density of states for the icosahedral alloys studied to date.[2-4] This is not entirely unexpected since these powder measurements represent an orientational average of all modes along all directions convoluted with the instrumental resolution.

In the last two years, several groups have attempted calculations of the full wave-vector and frequency-dependent response function $S(\mathbf{Q},\omega)$ for one-, two-, and three-dimensional quasilattices. Although most of this work describes calculations of spin dynamics (magnons) on a quasilattice, the results carry over directly to vibrational excitations (phonons) by the transformation $\omega \rightarrow \omega^2$. These studies have resulted in several specific predictions for the behavior of phonon modes in quasicrystals that may be tested by inelastic-neutron-scattering measurements.

Patel and Sherrington[25] calculated $S(\mathbf{Q},\omega)$ for a system of ferromagnetically coupled spins on 4181 sites of a two-dimensional Penrose tiling. They found well-defined propagating spin-waves with isotropic dispersion close to the zone centers (Bragg peaks) of the quasilattice. The energy widths of the excitations were consistent with expectations based upon the resolution of the calculation and finite size of the tiling. Furthermore, the integrated intensity of the excitations scaled linearly with the integrated intensity of their associated Bragg peaks.

The behavior of $S(\mathbf{Q},\omega)$ beyond the long-wavelength ($\mathbf{q} \rightarrow \mathbf{0}$) limit has been studied by several groups. For the one-dimensional Fibonacci sequence, Ashraff, Luck, and Stinchcombe derived an analytical expression for $S(\mathbf{Q},\omega)$ in the equal-coupling limit ($J_A = J_B$ in Fig. 1).[26,27] In this case the magnon dispersion consists of a main branch accompanied by many satellite branches of much lower intensity (Fig. 2). The strongest branch is associated with the strongest zone center. The satellite branches originate from other nearby zone centers of weaker intensity. In principle, there are an infinite number of satellite dispersion curves, since the reciprocal space is densely filled with zone centers, although most of these carry negligible spectral weight. In the equal-coupling limit, these branches cross without opening gaps. However, once the couplings between sites separated by different lengths are assigned different strengths ($J_A \neq J_B$), gaps open at the crossing points and increase in size as the difference between J_A and J_B increases. The resulting picture for the magnon- (or, equivalently, phonon-) dispersion curves consists of propagating modes at small wave vectors separated by a set of gaps from stripes of dispersionless modes at higher frequency. Similar features are observed in the phonon $S(\mathbf{Q},\omega)$ for a one-dimensional Fibonacci sequence obtained by the spectral-moments method[28] by Benoit, Poussigue, and Azougarh.[29] "Pseudo" dispersion curves[30] at small phonon wave vectors are observed for the most intense zone centers and are separated by a gap from higher-frequency dispersionless bands of scattering. By studying the Fourier transform of the time-dependent displacement-displacement correlation function, they also found that the higher-frequency modes are significantly more localized than the acoustic modes.

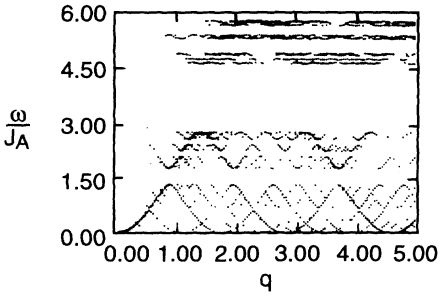

FIG. 2. Dispersion curves for spin waves on a Fibonacci sequence for $J_B/J_A = 2$ (after Ref. 26). The density of spots is proportional to the spectral weight of the inelastic excitation at that energy and wave vector.

One of the most interesting features of all of these calculations is the appearance of what might be termed "quasi"-Brillouin-zones. These are most clearly seen in regions of reciprocal space between pairs of strong Bragg peaks. In such cases the acoustic branches reach a maximum at the "quasi"-Brillouin-zone boundary (see Fig. 2). For three-dimensional icosahedral structures, Niizeki and Akamatsu have assigned these apparent zone boundaries to high-symmetry "special" points in the icosahedral reciprocal lattice.[31] The positions of these special points can be related to high-symmetry points in the six-dimensional hypercubic lattice, which is the parent of the icosahedral phase.[31,32]

As shown by Patel and Sherrington[25] and Ashraff, Luck, and Stinchcombe,[27] this same basic picture for the behavior of $S(\mathbf{Q},\omega)$ also seems to hold for two-dimensional Fibonacci lattices. However, it is interesting that calculations by the latter group, using the same numerical methods for a two-dimensional Penrose lattice, offer little evidence for well-defined phonon dispersion beyond the hydrodynamic regime. Therefore it is not entirely clear whether one should expect to see well-defined propagating phonon modes at large wave vectors for real three-dimensional icosahedral alloys.

It is also important to note that all of the calculations described above ignore the atomic decoration of the quasilattice. Although qualitative trends in the calculated $S(\mathbf{Q},\omega)$ may be compared with the results of neutron-

FIG. 1. Fibonacci sequence of atoms in one dimension. Atoms are separated by distances a or τa. The coupling parameters J_A and J_B are described in the text.

scattering experiments, quantitative comparisons cannot be made. One approach to the determination of $S(\mathbf{Q},\omega)$ for real quasicrystals is suggested by the existence of so-called crystalline approximants to the quasicrystalline alloys. These are large unit-cell periodic structures with internal icosahedral symmetry. For instance, the cubic R phase of Al-Li-Cu may be characterized as a body-centered-cubic packing of icosahedral clusters of atoms.[33–35] The icosahedral phase of Al-Li-Cu may be viewed as an aperiodic[36,37] or disordered[38] packing of these same clusters. An extensive study of the atomic structure of the icosahedral phase has been carried out by neutron and x-ray diffraction and six-dimensional crystallographic analysis.[39] This led to a model, in good agreement with the available data, that showed that the same icosahedral clusters exist in both the cubic and icosahedral phases. Knowledge of $S(\mathbf{Q},\omega)$ for the R phase, then, can provide a good starting point for realistic calculations of the response function for the icosahedral alloy.[40,41]

In this paper we describe inelastic-neutron-scattering measurements on single grains of icosahedral Al-Li-Cu and the closely related cubic R phase. Some results for the icosahedral alloy have been published previously.[5] In Sec. II the characterization of the single-grain specimens of the icosahedral and cubic R phases is described, and a reciprocal-space map of the region probed in these measurements is described. In Sec. III details of the instrumental configuration, data acquisition, and analysis are given. In Sec. IV we describe the results of our measurements of elastic isotropy in the icosahedral phase, the scaling of phonon intensities with the intensity of associated zone centers, and a comparison of the dispersion curves of the periodic and quasiperiodic samples. Where appropriate, our results are compared with the predictions of relevant dynamical models for quasicrystals.

II. SAMPLE CHARACTERIZATION

A 0.4-g single grain of icosahedral $Al_{60.3}Li_{29.2}Cu_{10.5}$ was extracted from a 2-kg ingot prepared by methods described elsewhere.[42] The grain is irregularly shaped with the approximate dimensions 8 mm × 6 mm × 4 mm, as shown in Fig. 3. Scanning electron microscopy showed that the surface of the grain is composed of oriented dendrites and clusters of oriented rhombic-triacontahedral crystallites. A collection of these faceted small grains is shown in Fig. 4; individual grains are on the order of 100 μm in size.

Neutron Laue photographs of the grain displayed only a single set of diffraction spots. The size and shape of the diffraction spots indicate that the entire grain contributes to the diffraction. No evidence of coherent scattering from second-phase inclusions were found in the neutron- and x-ray-diffraction scans of the grain. The mosaic of the sample was, however, relatively broad [1.2° full width at half maximum (FWHM)].

A 1.3-g grain of cubic $Al_{56}Li_{32}Cu_{12}$ was extracted from a 5-kg ingot prepared by methods described elsewhere.[43,44] The crystal, which was 8 mm × 7 mm × 10 mm in size, exhibits a [110] truncated cubic morphology. Neutron Laue photographs, however, showed that the crystal is twinned and consists of two grains of approximately the same size with the [221] direction of one parallel to the [100] direction of the other. During the inelastic-scattering experiment, care was taken, where possible, to avoid regions of reciprocal space where strong spots of both grains are nearby.

The icosahedral phase sample was oriented such that a twofold plane, shown schematically in Fig. 5, was coincident with the scattering plane in order to facilitate measurements along the high-symmetry twofold, threefold, and fivefold axes. The R-phase sample was oriented so

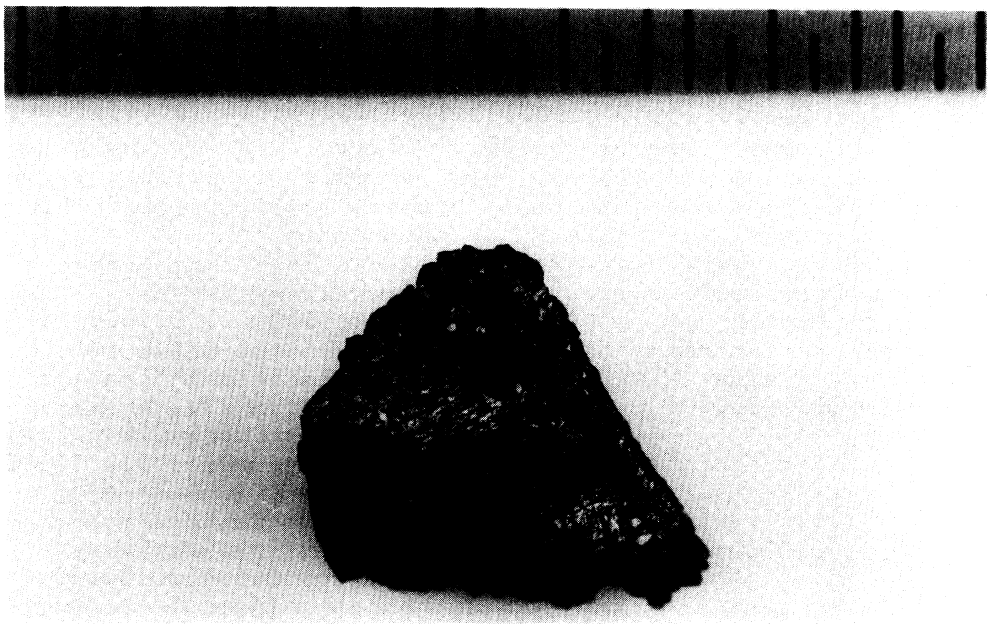

FIG. 3. Grain of icosahedral Al-Li-Cu used in the present measurements. The scale at the top is in millimeters.

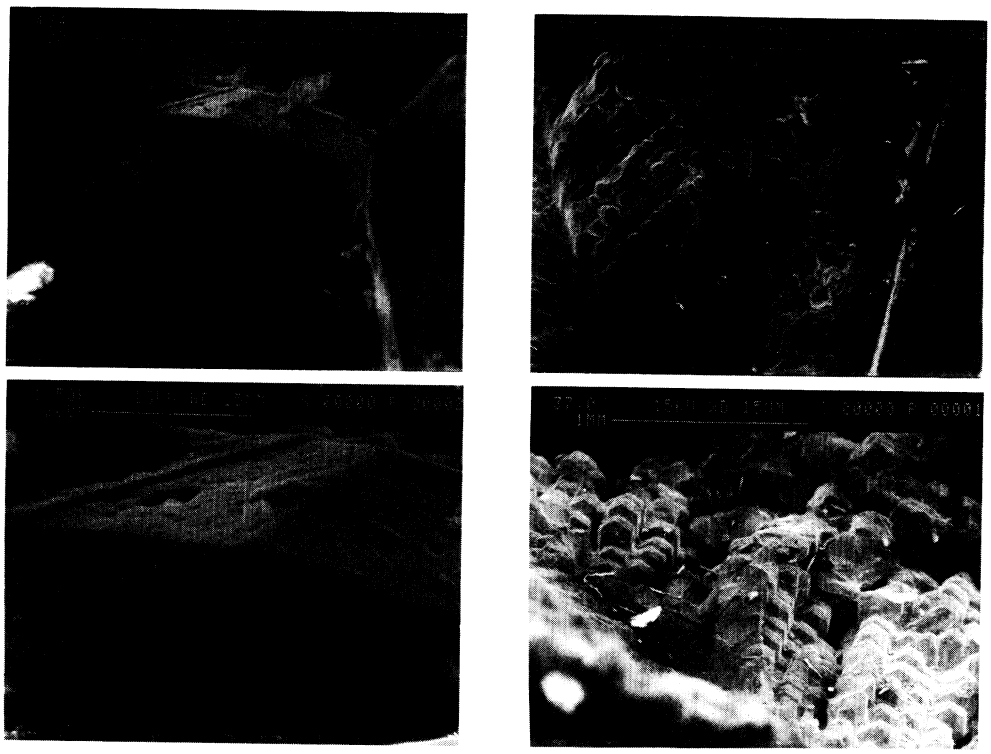

FIG. 4. Scanning-electron-microscope (SEM) photographs of the grain in Fig. 2, showing the microstructure of the surface. The scale of features is indicated in each photograph.

that the analogous twofold plane of the larger grain was coincident with the scattering plane (also shown in Fig. 5). The areas of the circles in these plots are proportional to the measured or calculated[39] intensities of the respective elastic-scattering peaks. In the schematic of the twofold plane for the cubic R phase, arrows denoting the threefold and fivefold axes of the icosahedral phase have been included to emphasize the close similarity of the two diffraction patterns. Although the pattern of diffraction spots for the R phase is periodic, the intensity modulations of the pattern bear a strong resemblance to those of the icosahedral phase. This results from the fact that the dominant scattering clusters in the cubic unit cell of the R phase have icosahedral symmetry.

Figure 6 shows elastic scans taken along the dashed lines in Fig. 5 for both the icosahedral- and R-phase samples. The top panel describes a scan perpendicular to the momentum transfer $\mathbf{Q}$ and so measures the relative mosaicity of the two samples. We also see here that the R-phase sample scan exhibits additional peaks which are due to the presence of the second grain. Care was taken to isolate the inelastic-scattering contribution of this second grain. In all instances the phonon groups associated with Bragg peaks from the second grain were easily distinguished from the excitations due to the primary grain.

The phonon wave vector corresponding to inelastic measurements is defined by the relation $\mathbf{q}=\mathbf{Q}-\mathbf{G}$, where $\mathbf{Q}$ is the momentum transfer, $\mathbf{k}_F-\mathbf{k}_I$, and $\mathbf{G}$ is the reciprocal-lattice vector of the zone center (Bragg peak) chosen as the origin for the measurement. Since the reciprocal space of the icosahedral phase is aperiodic, all wave vectors are labeled in units of Å^{-1}, rather than reciprocal-lattice units as is typically done for periodic crystals. For reference, the Miller indices for a few of the diffraction spots of the R phase are given in Fig. 5. Some icosahedral phase peaks are labeled by letters A–K. The icosahedral indices corresponding to these labels are given in Table I.

III. INELASTIC-NEUTRON-SCATTERING MEASUREMENTS

Most of the inelastic-neutron-scattering measurements described in this paper were made on the IN8 triple-axis spectrometer at the Institute Laue-Langevin (ILL) using a vertically bent copper (111) monochromator and a vertically bent pyrolytic graphite (PG) (002) analyzer. Constant-Q scans were performed at a fixed final neutron energy of 44.8 meV, and collimations of 50′-40′-40′-40′, numbers (in units of arc min) which refer to the horizontal collimations of the beam between the reactor and monochromator, monochromator and sample, sample and analyzer, and analyzer and detector, respectively. This configuration was chosen so that the (E-q) slope of the instrumental resolution function was as close as possible to the slope of the transverse-acoustic-phonon branch to maximize the effect of focusing.[45] The instrumental contribution to the measured phonon width in this case is about 3 meV. For longitudinal modes, where there is no focusing effect, as well as for the higher-energy range of the transverse branches where the dispersion curves bend

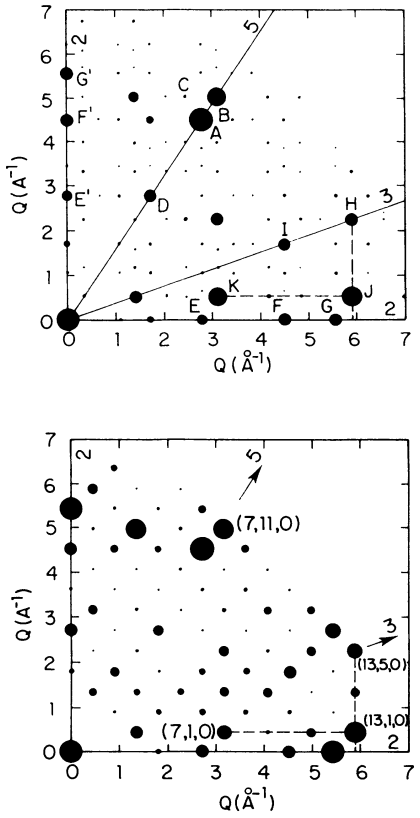

FIG. 5. Twofold planes for the icosahedral (top) and *R* phase (bottom) of Al-Li-Cu investigated in these measurements. The dashed lines denote the directions of elastic scans in Fig. 6, as well as the region of inelastic-scattering measurements for the twofold longitudinal and transverse modes as described in Sec. III C. Letters in the top panel refer to zone centers listed in Table I. The arrows in the bottom panel denote the threefold and fivefold axes of the icosahedral phase for comparison.

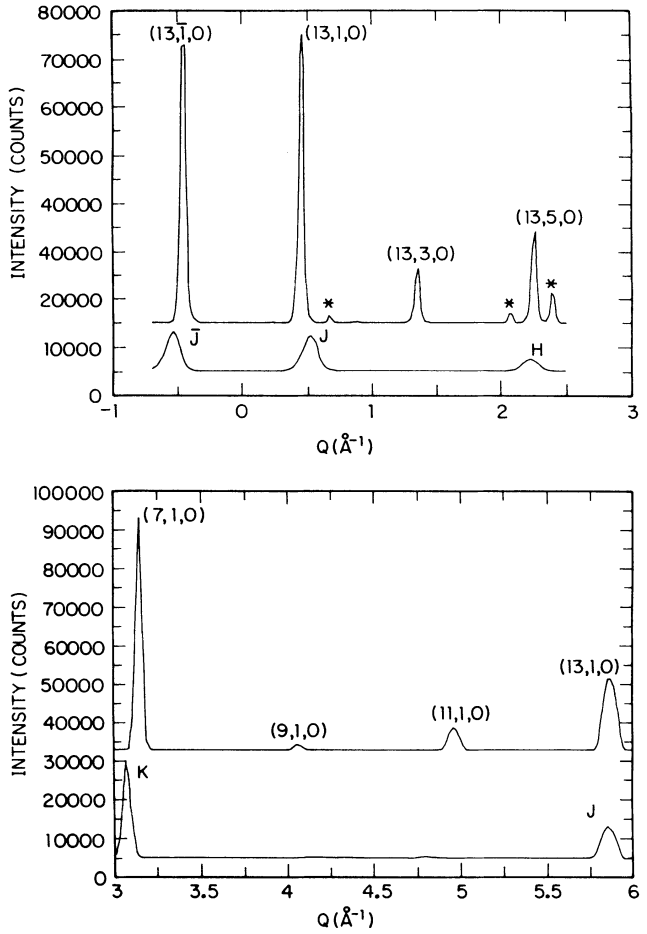

FIG. 6. Elastic scans along the dashed lines in Fig. 5 for both the *R*-phase (top trace) and icosahedral (bottom trace) alloys. The peaks marked with an asterisk are due to a second *R*-phase grain in the sample, with a different orientation from the primary grain used in the inelastic measurements.

over, the energy width of phonon peaks is of the order of 5 meV. Measurements of the low-energy acoustic modes, at small **q**, were made at IN8 using a fixed final energy of 14.7 meV, the same collimation, and a pyrolytic graphite filter to eliminate higher-harmonic contamination of the scattered beam.

TABLE I. Zone centers used for neutron-scattering measurements.

Label	$\lvert\mathbf{G}\rvert=\lvert\mathbf{G}_\parallel\rvert$ (Å^{-1})	$\lvert\mathbf{G}_\perp\rvert$ (Å^{-1})	Indices	*R*-phase analog
A	5.26	0.33	(42222$\bar{2}$)	(6,10,0)
B	5.89	0.37	(52222$\bar{2}$)	(7,11,0)
C	5.57	0.91	(242$\bar{2}$32)	(5,11,0)
D	2.63	0.17	(21111$\bar{1}$)	(4,6,0)
E	2.77	0.28	(120$\bar{1}$20)	(6,0,0)
F	4.48	0.17	(230$\bar{2}$30)	(10,0,0)
G	5.54	0.57	(240$\bar{2}$40)	(12,0,0)
H	6.28	0.09	(444111)	(13,5,0)
I	4.79	0.49	(331$\bar{1}$3$\bar{1}$)	(10,4,0)
J	5.89	0.37	(340$\bar{2}$40)	(13,1,0)
K	3.14	0.49	(220$\bar{1}$20)	(7,1,0)

In addition to the measurements made at the ILL, data were taken on the thermal-neutron 2T and cold-neutron 4F2 triple-axis spectrometers of the Laboratoire Léon Brillouin at Saclay, France. In the 2T spectrometer, doubly bent Cu(111) crystals were used as the monochromator and analyzer. No collimation, beyond that provided by the beam-transport tubes, was employed in order to take full advantage of the focusing capabilities of the instrument. The effective collimation of the beam was estimated to be 60′-200′-90′-70′. For the low-lying transverse-acoustic modes, the energy width of the resolution function, at a fixed final neutron energy of 42 meV, is not significantly larger than that found using tighter collimation at IN8. On the other hand, longitudinal modes measured on 2T were significantly broader than those measured at IN8. Some preliminary measurements on the 4F2 triple axis were done at a fixed incident energy of 5 meV in order to study the low (≤ 1 meV) excitations at very small phonon wave vectors.

Constant-Q energy scans of the icosahedral phase sample were taken along the twofold, threefold, and fivefold directions. Frequently, excitations were measured from

several zone centers in order to check for consistency in frequency and intensity. A more complete map of the low-lying phonon modes along the twofold direction was taken between points J and H (transverse polarization) and points J and K (longitudinal polarization), as well as from point G. Similarly, the phonon dispersion between the (13,1,0), (13,5,0), and (7,1,0) reciprocal-lattice points and near the (12,0,0) Bragg point in the cubic R phase were determined for comparison with the icosahedral-phase data.

In Fig. 7 we show constant-Q scans through neutron groups taken at $\mathbf{Q}=(5.86,1.38,0)$ and $\mathbf{Q}=(5.86,1.25,0)$ for the icosahedral- and R-phase samples, respectively. These positions correspond to phonon wave vectors with a magnitude of 0.85 and 0.8 Å^{-1} from peak J (icosahedral phase) and the (13,1,0) peak of the R phase, respectively. As shown in the insets of Fig. 7, the momentum transfer ($\mathbf{Q}$) is nearly perpendicular to the phonon wave vector ($\mathbf{q}$). Therefore these scans probe modes of transverse polarization along the twofold axis.

The inelastic-scattering data for both samples contain contributions from air scattering, substantial incoherent scattering from Li, and scattering from the aluminum sample holder, in addition to the phonon excitations of interest. The air-scattering contribution is well described by a Gaussian with a width of 31 meV (FWHM) at $Q=5.5$ Å^{-1}. For the data discussed below, a straight-line fit to the background proved sufficient for modeling the background over a range of neutron-energy loss from 3 to 20 meV (see dashed line in Fig. 7). The slope and intercept of this line were fixed at the same values during fits to both the R- and icosahedral-phase phonon peaks. Fits to the phonon peaks were initially done using a damped harmonic-oscillator line shape convoluted with the spectrometer-resolution function. However, it was found that the instrumental energy width was broader than the intrinsic width of the excitations. Therefore a simple normalized Gaussian with a width fixed to the instrumental resolution was employed to determine the position and intensity of the phonon groups.

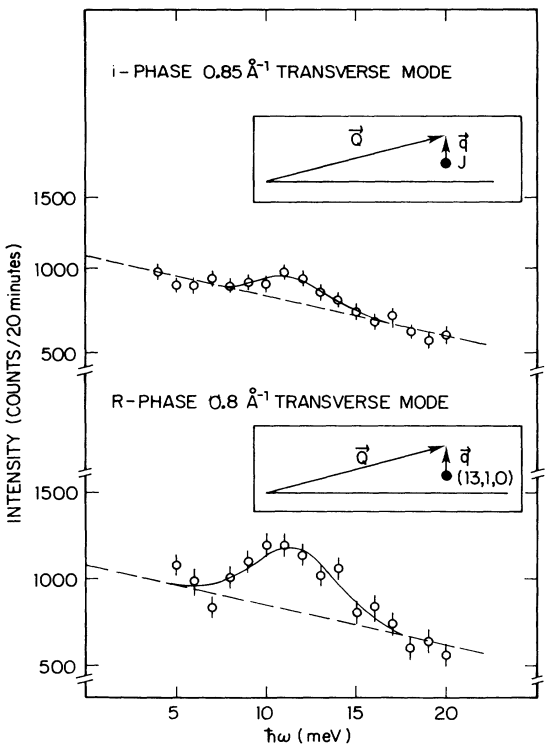

FIG. 7. Twofold transverse phonon groups for the icosahedral and R-phase samples. The dashed line indicates the air-scattering contribution, while the solid lines describe the fit to the phonon peaks using a Gaussian with a width fixed at the resolution of the instrument. The insets show the scattering geometry for these measurements.

IV. RESULTS AND DISCUSSION

In the following sections, we describe the results of these measurements and their relationship to our current understanding of the dynamics of icosahedral quasiperiodic systems.

A. Isotropic dispersion of the long-wavelength acoustic modes

In the long-wavelength limit ($|\mathbf{q}|\rightarrow 0$), the slopes of the dispersion curves may be related to sound velocities determined by ultrasonic measurements using

$$\omega=\frac{E}{\hbar}=v_j|\mathbf{q}| \ , \tag{1}$$

where v_j is the appropriate longitudinal- or transverse-sound velocity. Ultrasonic measurements by Reynolds *et al.* on single grains of icosahedral Al-Li-Cu found that $v_L=(6.4\pm0.1)\times10^5$ cm/s and $v_T=(3.8\pm0.1)\times10^5$ cm/s along both the twofold and fivefold axes.[46]

The points in Fig. 8 represent the peak centroids of phonon groups taken along the high-symmetry twofold, threefold, and fivefold axes of the icosahedral-phase sample. Within experimental error the dispersion relations for both longitudinal and transverse modes out to phonon wave vectors of 0.2–0.3 Å^{-1} are independent of direction. We also point out that measurements of the transverse-acoustic phonons along the pair of twofold directions, separated by 90° in the twofold plane, probe modes of different polarizations and were found to be indistinguishable.

The solid lines in Fig. 8 represent the extrapolated linear dispersion calculated from Eq. (1) using the sound velocities determined by Reynolds *et al.* There is clearly excellent agreement between the initial slope of the dispersion curve extrapolated from the ultrasonic data and the neutron-scattering data.

Unfortunately, because of time constraints, we were not able to complete a full set of similar measurements, at small $\mathbf{q}$, on the R-phase sample. In previous work on the IN14 triple-axis spectrometer, however, the transverse-acoustic modes propagating along a [011] direction were measured around the (600) and ($\bar{6}40$) reflections in the (01$\bar{1}$) and (001) zones, respectively.[47] This allows a comparison of transverse modes with [100] and [01$\bar{1}$] polarizations. In the first case, the sound velocity is given by

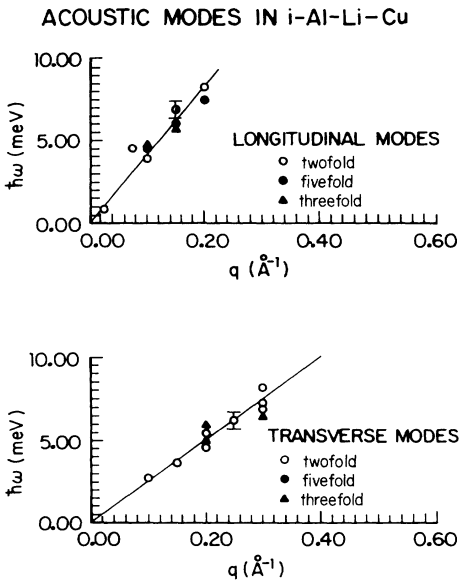

FIG. 8. Low-energy acoustic modes along the twofold, threefold, and fivefold axes for icosahedral Al-Li-Cu. The solid lines describe the extrapolated initial slopes of the dispersion curves using sound velocities from ultrasonic measurements as described in the text.

$v_{T_1}=\sqrt{c_{44}/\rho}$, where ρ is the density of the material. For the second case, $v_{T_2}=v_{T_1}/\sqrt{A}$, where the anisotropy factor A is given by $2c_{44}/(c_{11}-c_{12})$. As pointed out in the Introduction, for icosahedral symmetry, $A=1$. Even for the cubic crystal, as shown by the acoustic dispersion in Fig. 9, no anisotropy can be detected. The measured transverse-sound velocity for the cubic phase is 3.8×10^5 cm/s, the same as for the icosahedral phase.

In principle, the elastic isotropy of icosahedral alloys may be broken by the existence of phason modes.[12] In the absence of strong phason-phonon interactions, the phason contribution to the longitudinal and transverse-sound frequencies appears as a damping term which should broaden the inelastic excitations anisotropically, revealing the icosahedral symmetry of the structure. The

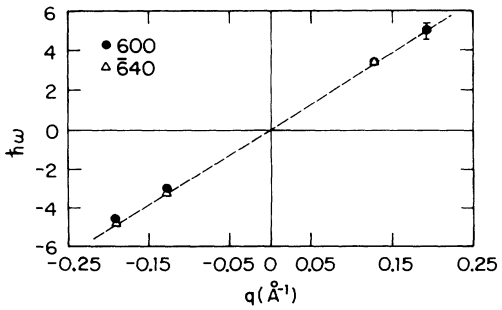

FIG. 9. Dispersion relation for transverse-acoustic modes propagating in the [001] direction with [100] (solid circles) and [01$\bar{1}$] (triangles) polarization. Positive and negative energies correspond to measurements made for neutron-energy loss and gain, respectively.

frequencies of the modes themselves may be altered by strong phason-phonon coupling. Our measurements here, as well as the ultrasonic measurements on Al-Li-Cu (Ref. 46) and recent inelastic-neutron-scattering measurements on icosahedral Al-Cu-Fe,[6] find no evidence of strong phonon-phason coupling in Al-Li-Cu, since the dispersion of acoustic modes along the high-symmetry (and other) directions is isotropic. Unfortunately, the relative large breadth of the instrumental energy resolution did not permit a sensitive test of the presence of anisotropy in the phonon excitation widths. However, for diffusive phason modes the ratio of the anisotropic to isotropic damping contribution has been estimated to be on the order of $D/\eta\sim10^{-10}$, where D is the vacancy-diffusion constant for the alloy and η is the viscosity of the medium.[12] For pinned phason dynamics, no contribution is expected below the depinning temperature. It is widely believed that phason dynamics in systems such as Al-Mn, Al-Li-Cu, and most other icosahedral alloys are pinned at room temperature, and perhaps at all temperatures below the melting point since phason strain cannot be annealed by prolonged heat treatment at elevated temperatures. Therefore it is highly unlikely that anisotropic phonon-peak broadening or softening due to phason contributions is expected to be significant. Interestingly, this may not be the case for the face-centered icosahedral (FCI) alloy of Al-Cu-Fe since there is now some evidence that phason modes are active at high temperatures.[48–53]

B. Scaling properties of acoustic-phonon intensities

The inelastic-neutron-scattering cross section is given by[54]

$$\frac{d^2\sigma}{d\omega\, d\Omega}=\frac{k_F}{k_I}S(\mathbf{Q},\omega)\ , \tag{2}$$

where k_F and k_I are the magnitude of the final and incident neutrons wave vectors, respectively. $S(\mathbf{Q},\omega)$ is the dynamical scattering factor described in the Introduction. For scattering of the neutron to a final state, characterized by a wave vector k_F and energy $(h^2/2m)k_F^2$, due to the creation or annihilation of a phonon of frequency ω_j and wave vector $\mathbf{q}$,

$$S(\mathbf{Q},\omega)=\frac{\langle n(\omega)+\frac{1}{2}\pm\frac{1}{2}\rangle}{\omega_j(\mathbf{q})}|F_{\rm in}(\mathbf{Q})|^2 \times\delta(\hbar\omega_F-\hbar\omega_I\pm h\omega_j(\mathbf{q}))\delta(\mathbf{Q}\pm\mathbf{q}-\mathbf{G})\ . \tag{3}$$

The first term in angular brackets describes the phonon population at temperature T, with the upper and lower signs corresponding to phonon creation and annihilation, respectively; the two δ functions assure conservation of energy and momentum. For crystalline solids the inelastic-structure factor $F_{\rm in}(\mathbf{Q})$ involves a sum taken over all atoms in a unit cell:

$$F_{\rm in}(\mathbf{Q})=\sum_k M_k^{-1/2}b_k\hat{\mathbf{e}}_k^j(\mathbf{q})\cdot\mathbf{Q}e^{i\mathbf{Q}\cdot\mathbf{d}_k}e^{-W}\ . \tag{4}$$

Here b_k is the neutron-scattering length for atom k in the unit cell and $\hat{\mathbf{e}}_k^j$ is the polarization of the jth mode. For

quasicrystals the calculation of the inelastic-structure factor is tremendously complicated by the absence of a finite-size unit cell and, therefore, sufficient knowledge of the atomic positions. The summation, in principle, must extend over all atoms in the grain.

Qualitatively, at least, we may determine whether or not the quasicrystal phonon data follows the same general scaling relation observed for periodic crystals. If we expand the exponential term in Eq. (3) and keep terms to first order, for small **q** (close to a zone center), the inelastic-structure factor for acoustic modes increases in proportion to the static-structure factor and, hence, the integrated intensity of the Bragg scattering. At constant ω the phonon cross section for different zone centers should follow:

$$\frac{d^2\sigma}{d\omega\, d\Omega} \sim F^2_{\text{static}} Q^2_{\parallel} , \tag{5}$$

where $Q_{\parallel}$ is the component of **Q** along the polarization vector. To test this a set of transverse modes along the twofold axis, 0.3 Å^{-1} from zone centers *J*, *A*, *H*, *F*, and *G*, was measured. Figure 10 displays the phonon intensities, normalized by Q^2, as a function of the integrated intensity of their respective zone centers. We find that the Bragg-peak intensity is directly proportional to the square of the static-structure factor as determined by de Boissieu *et al.* from neutron-powder-diffraction measurements of icosahedral Al-Li-Cu,[39] in agreement with the predictions of Patel and Sherrington[25] and Benoit, Poussigue, and Azougarh,[29] as well as the expectations derived from the discussion above.

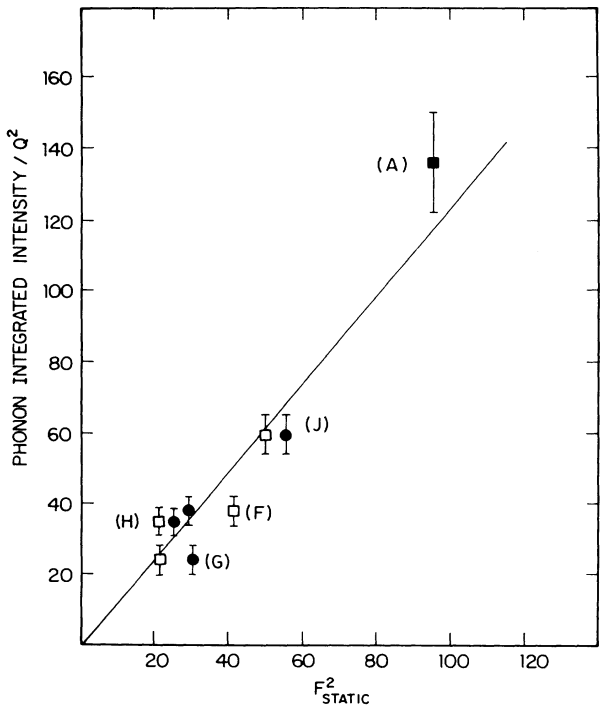

FIG. 10. Dependence of phonon-integrated intensity upon the integrated intensity of the zone-center Bragg peak (open squares) or the static-structure factor obtained from Ref. 42 (solid circles). Both measures of F_{static} are normalized at the highest value of the calculated F_{static}. Letters denote the zone center for the measurements, and the solid line is a guide to the eye.

It is worth emphasizing here that the Al-Li-Cu icosahedral alloy exhibits measurable phason strain.[15] For elastic scattering the signature of this particular form of disorder is diffraction-peak broadening which increases linearly with the magnitude of the phason momentum $G_{\perp}$ associated with the zone center, rather than the magnitude of its reciprocal-lattice vector $G_{\parallel}$, as is found for strain broadening in periodic crystals.[14] Table I contains both the $G_{\parallel}$ and $G_{\perp}$ values for zone centers probed in this measurement.

Benoit, Poussigue, and Azougarh have studied the effect of disorder upon the intensity and positions of phonon groups for a one-dimensional Fibonacci sequence by randomly changing bonds ($S \rightarrow L$ and $L \rightarrow S$) in their calculations.[29] This operation essentially introduces "phase" defects and so is analogous to the phason-strain disorder in real quasicrystals. They observed that the intensity of acoustic modes decreased strongly upon increasing the number of these types of defects, more strongly for phonon groups associated with the weaker-diffraction peaks (higher $G_{\perp}$) than for the strong-diffraction peaks (lower $G_{\perp}$). The data in Fig. 10 include zone centers which cover a range of $G_{\perp}$ values. No systematic dependence of phonon intensity with the phason momentum of the zone center, beyond that associated with the static-structure factor of the elastic scattering, was observed.

C. Dispersion curves for the icosahedral- and *R*-phase alloys

In order to compare the dispersion relations for the icosahedral- and *R*-phase samples, scans of transverse and longitudinal modes along the twofold axis were taken along the directions indicated by dashed lines in Fig. 5. These particular regions were selected because they cover approximately the same range of reciprocal space for both samples and because the sequence of elastic-scattering peaks, both in position and intensity, are quite similar.

In Fig. 11 we show the transverse phonon dispersion along the twofold direction for the icosahedral- and *R*-phase samples. Figures 12 and 13 show the longitudinal phonon dispersion along the twofold axes for both samples. These data correspond to the centroids of neutron groups obtained in a constant-**q** energy scans over a range from 2 to 18 meV. Symmetry points for the cubic *R* phase are labeled using the conventional group-theoretic notation, along with the identification of the Bragg point corresponding to the zone center.

For the icosahedral-phase sample, the behavior of the transverse phonon dispersion along the twofold axis, as well as previously reported results for longitudinal modes along the fivefold axis (Fig. 14), suggest that one can define quasi-Brillouin-zones in the reciprocal space of the icosahedral phase between pairs of strong Γ points as predicted by several theoretical calculations of $S(\mathbf{Q},\omega)$.

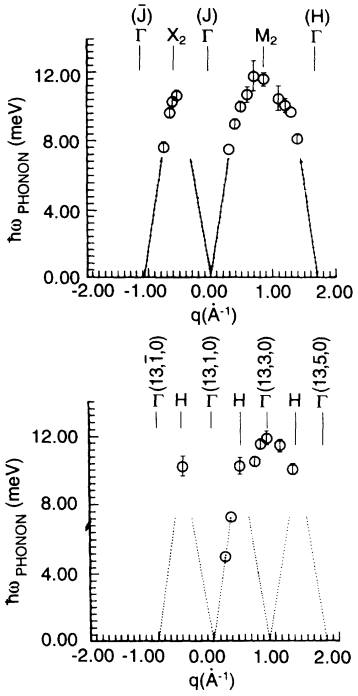

FIG. 11. Transverse phonon modes along the twofold directions for icosahedral (top panel) and the cubic R phase (bottom panel) of Al-Li-Cu. The Γ points denote the zone-center positions, while other special points are described in the text. The dotted lines indicate the low-energy acoustic-mode dispersion. Zone centers are labeled by their Miller indices or letters (see Table I).

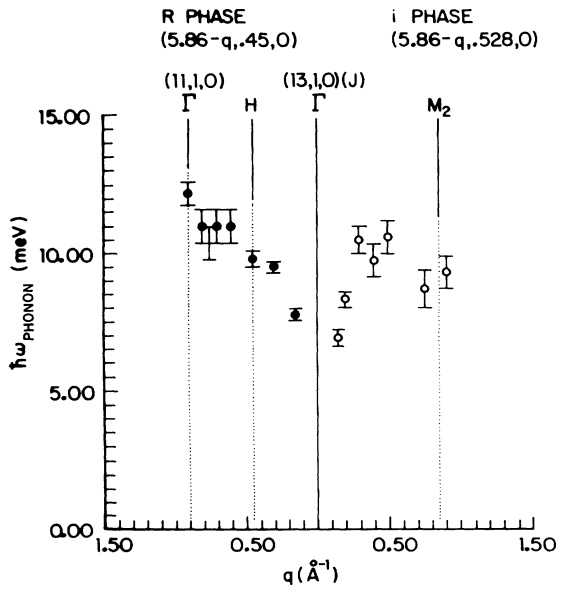

FIG. 12. Longitudinal phonon dispersion along a twofold direction for the icosahedral phase measured from point J (right side) and R phase, measured from the (13,1,0) (left side). Dotted lines signify special points in reciprocal space as described in the text.

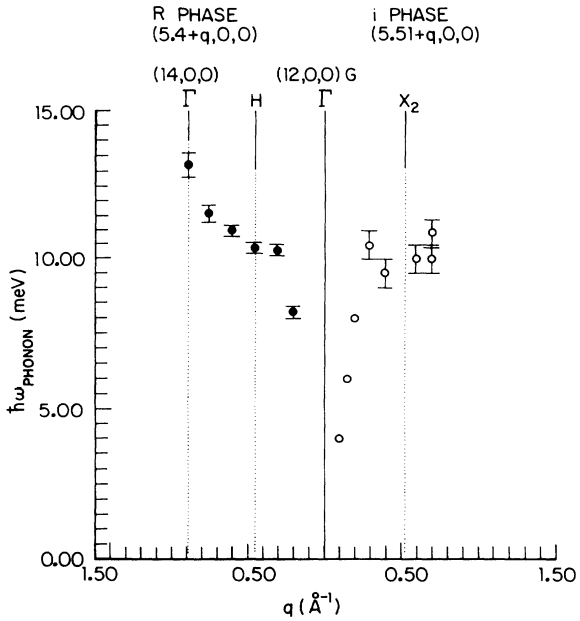

FIG. 13. Longitudinal phonon dispersion along a twofold direction for the icosahedral phase measured from point G (right side) and R phase, measured from the (12,0,0) (left side). Dotted lines signify special points in reciprocal space as described in the text.

Although, in principle, the concept of Brillouin zones is ill defined for quasiperiodic structures, operationally one may identify "quasizones" between the most intense zone centers.

The positions denoted as Γ, M_2, X_2, and M_5 in Figs. 11–14 for the icosahedral phase represent the projection of the special points of a six-dimensional simple hypercubic lattice down onto the twofold plane of the icosahedral

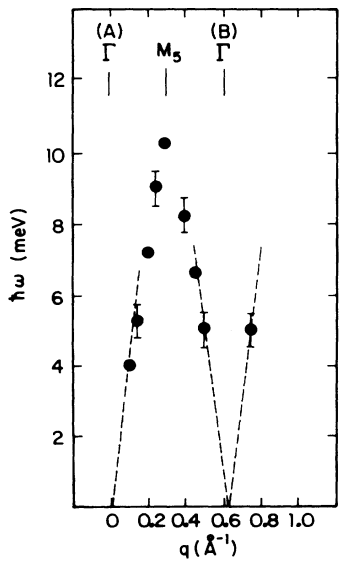

FIG. 14. Longitudinal modes along the fivefold axis between points A and B of the icosahedral phase (after Ref. 5).

phase as described by Niizeki and Akamatsu.[31,32] Briefly, these special points describe positions of high symmetry in the six-dimensional lattice of the form $\frac{1}{2}(n_1,n_2,n_3,n_4,n_5,n_6)$ where n_1-n_6 are integers.[55] For example, the Γ label denotes points where all n_i are even (zone centers), while the X_2 points are of the form $\frac{1}{2}(1,1,0,0,0,0)$. The physical significance of these special points is analogous to that for the corresponding special points in the reciprocal lattice of periodic crystals. They describe critical, or stationary, points of the dispersion relation for electronic or vibrational states where one would expect maxima in the dispersion curve, as are found in our measurements for icosahedral Al-Li-Cu.

Generally speaking, the longitudinal and transverse phonon-dispersion curves for the icosahedral and cubic R phases are quite similar. Indeed, as noted before, the long-wavelength acoustic dispersions along the twofold directions are essentially indistinguishable. This is not unexpected since at the long-wavelength (small $\mathbf{q}$) continuum limit, excitations are relatively insensitive to the details of the atomic structure of materials. At higher energy, at least for the transverse modes, there are also similarities in the form of the phonon dispersion for the icosahedral- and R-phase samples. This result is encouraging since it validates one approach to the determination of the inelastic-structure factor for real quasicrystalline systems: the extension of theoretical calculations of $S(\mathbf{Q},\omega)$ for the crystalline approximants.[40,41]

On the other hand, differences in the phonon dispersion between the two alloys (most clearly illustrated in Figs. 12 and 13) are found at higher energy for phonon wave vectors larger than about 0.4–0.5 Å^{-1}. The longitudinal modes of the R phase exhibit low-lying dispersive optical branches in the region $\Gamma \rightarrow H \rightarrow \Gamma$. In contrast, for the icosahedral-phase sample, the higher-energy longitudinal phonon excitations along the twofold axes appear as dispersionless branches which are quite similar to the localized excitations at higher energy found in the one- and two-dimensional calculations of $S(\mathbf{Q},\omega)$ for Fibonacci lattices (see Fig. 2). In fact, there is an interesting connection between the twofold direction of the icosahedral phase and the one-dimensional Fibonacci sequence. The twofold planes of the icosahedral phase are dense-packed layers, and as high-resolution electron microscopy images have shown, the atomic configurations along the twofold axis closely resemble a Fibonacci sequence of "atomic planes." This has also been proposed as an alternative way of viewing the quasicrystalline structure of Al-Li-Cu.[39] In terms of diffraction properties, we point out that the sequence of diffraction peaks along a twofold axis of the icosahedral phase is identical to the diffraction pattern from a one-dimensional Fibonacci sequence. Indeed, the close similarity between the diffraction patterns motivates a comparison of the longitudinal modes probed along a twofold direction with dynamical calculations for one-dimensional Fibonacci sequence.

While phonon DOS measurements of icosahedral Al-Li-Cu by Suck *et al.*[4] found maxima in the inelastic spectrum at 13, 16, and 21 meV, our own measurements on a single grain of icosahedral Al-Li-Cu found no distinct excitations at these energies.[56] Interestingly, the flat 10-meV mode found in our measurements does not appear as a distinct peak in the phonon DOS measurements. This means that the spectral weight carried by this mode must be smaller than that carried by other, perhaps more localized, modes at higher energy. Excitations which are spatially localized give rise to dispersionless scattering, which is distributed over a correspondingly large region in reciprocal space. The density-of-states measurement is more sensitive to the presence of localized modes since it makes use of powder samples, thereby averaging over all directions and phonon wave vectors, for some particular energy range. Other recent measurements of inelastic excitations in quasicrystals have had little success in finding the higher-energy opticlike modes in these systems. In icosahedral Al-Cu-Fe, for instance, excitations above 10 meV could not be observed.[6] Similarly, atomic-beam-scattering experiments on the decagonal phase of Al-Co-Ni found that surface phonon peaks broadened and diminished at higher energy (of the order of 10 meV).[57] All of the evidence cited above appears to point to an enhanced degree of localization for the higher-energy modes in quasiperiodic systems.

Finally, independent of any specific interpretation of behavior of the phonons in the icosahedral phase at higher energy and wave vector, we point out that it is precisely in this region that we should expect to see differences between the icosahedral- and R-phase samples. First, consider the measurements made on the R-phase sample. Inelastic-neutron-scattering experiments probe dynamical correlations between atoms over distances which vary inversely with $|\mathbf{q}|$. Very close to the zone center, dynamical effects over very large length scales compared with the size of the unit cell are probed. As $\mathbf{q}$ increases, dynamical correlations over smaller distances become more important until, at the zone boundary, we essentially probe the correlated motions between atoms on neighboring icosahedral clusters of atoms in the cubic unit cell of the R phase. As mentioned in the Introduction, some models for the icosahedral phase of Al-Li-Cu view the structure as an aperiodic or disordered packing of these same icosahedral clusters of atoms. Therefore differences in the behavior of excitations at phonon wave vectors ($\approx$0.4–0.5 Å) approaching intercluster separations ($\approx$12 Å) may be attributed to differences in the details of how these clusters are packed together.

V. SUMMARY

We have reported on inelastic-neutron-scattering measurements of single grains of the icosahedral and cubic R phases of Al-Li-Cu. Well-defined transverse- and longitudinal-acoustic branches are observed in the vicinity of strong Bragg reflections. For the icosahedral phase, the phonon dispersion at small and finite $\mathbf{q}$ is independent of direction, as expected for an isotropic solid, in agreement with previous ultrasonic measurements. In the somewhat more limited measurements of acoustic dispersion in the cubic R phase, we also find a high degree of elastic isotropy. Further measurements of the acoustic

branches for the cubic phase will be necessary in order to place limits on the degree of elastic anisotropy in this system. The special weight of the acoustic modes for the icosahedral phase scale linearly with the integrated intensity of the associated zone center as is found for three-dimensional periodic crystals. No systematic dependence of phonon intensity with the phason momentum of the zone center, beyond that associated with the static-structure factor of the elastic scattering, was observed. In particularly favorable instances, where the phonon dispersion is measured between two strong Bragg peaks, "quasizones" are observed. The stationary points of these zones may be identified as high-symmetry points in the icosahedral quasilattice which are special points in a related six-dimensional hypercubic lattice.

The general trends of the low-energy phonon dispersion for both the icosahedral- and R-phase alloys are quite similar. This suggests that it may indeed be possible to model the dynamical response of quasicrystalline alloys using the measured, or calculated, dynamical response of approximant phases. This approach could greatly reduce the difficulties inherent to first-principles methods currently being used. On the other hand, we also find differences in $S(\mathbf{Q},\omega)$ between the icosahedral phase and its cubic approximant at higher energies. Specifically, the higher-energy modes in the Al-Li-Cu quasicrystal are more localized than corresponding modes in the cubic phase.

ACKNOWLEDGMENTS

The authors wish to thank C. Benoit, B. N. Harmon, K. M. Ho, and M. Widom for their assistance and useful discussions. We thank B. Dubost (Pechiney Research Center, Voreppe) and C. Degand (Laboratorie de Physique des Solides, Orsay) for preparation of the R-phase Al-Li-Cu. One of us (A.I.G.) wishes to thank the ILL for its hospitality during the experiment. Ames Laboratory is operated for the U.S. Department of Energy by Iowa State University under Contract No. W-7405-ENG.

[1]For a recent review, see A. I. Goldman and M. Widom, Annu. Rev. Phys. Chem. **42**, 685 (1991).
[2]P. F. Micelli, S. E. Youngquist, D. A. Neumann, H. Zabel, J. J. Rush, and J. M. Rowe, Phys. Rev. B **34**, 8977 (1986).
[3]J.-B. Suck, H. Bretscher, H. Rudin, P. Grütter, and H.-J. Güntherodt, Phys. Rev. Lett. **59**, 102 (1987).
[4]J.-B. Suck, C. Janot, M. De Boissieu, and B. Dubost, in *Phonons '89,* edited by S. Hunklinger, W. Ludwig, and G. Weiss (World Scientific, Singapore, 1990), pp. 576–578.
[5]A. I. Goldman, C. Stassis, R. Bellissent, H. Moudden, N. Pyka, and F. W. Gayle, Phys. Rev. B **43**, 8763 (1991).
[6]M. Quillichini, G. Heger, B. Hennion, S. Lefebvre, and A. Quivy, J. Phys. (Paris) **51**, 1785 (1990).
[7]L. C. Chen, S. Ebalard, L. M. Goldman, W. Ohashi, B. Park, and F. Spaepen, J. Appl. Phys. **60**, 2683 (1986).
[8]P. A. Kalugin, A. Y. Kitaev, and L. S. Levitov, Pis'ma Zh. Eksp. Teor. Fiz. **41**, 119 (1985) [JETP Lett. **41**, 145 (1985)].
[9]P. Bak, Phys. Rev. Lett. **54**, 1517 (1985); Phys. Rev. B **32**, 5764 (1985).
[10]D. Levine, T. C. Lubensky, S. Ostlund, S. Ramaswamy, P. J. Steinhardt, and J. Toner, Phys. Rev. Lett. **54**, 1520 (1985).
[11]J. D. Axe and P. Bak, Phys. Rev. B **26**, 4963 (1982).
[12]For example, see T. C. Lubensky, in *Introduction to Quasicrystals,* edited by M. V. Jaric (Academic, San Diego, 1988), pp. 199–280.
[13]T. C. Lubensky, J. E. S. Socolar, P. J. Steinhardt, P. A. Bancel, and P. A. Heiney, Phys. Rev. Lett. **57**, 1440 (1986).
[14]P. M. Horn, W. Malzfeldt, D. P. Divincenzo, J. Toner, and R. Gambino, Phys. Rev. Lett. **57**, 1444 (1986).
[15]P. A. Heiney, P. A. Bancel, P. M. Horn, J. L. Jordan, S. LaPlaca, J. Angilello, and F. W. Gayle, Science **238**, 660 (1987).
[16]N. O. Birge, B. Golding, W. H. Harmmerle, H. S. Chen, and J. M. Parsey, Jr., Phys. Rev. B **36**, 7685 (1985).
[17]M. Kohmoto, L. P. Kadanoff, and C. Tang, Phys. Rev. Lett. **50**, 1870 (1983).
[18]S. Ostlund and R. Pandit, Phys. Rev. B **29**, 1394 (1984).
[19]T. C. Choy, Phys. Rev. Lett. **55**, 2915 (1985).
[20]J. M. Luck and D. Petritis, J. Stat. Phys. **42**, 289 (1986).
[21]J. P. Lu, T. Odagaki, and J. L. Birman, Phys. Rev. B **33**, 4809 (1986).
[22]F. Nori and J. P. Rodriguez, Phys. Rev. B **34**, 2207 (1986).
[23]M. Kohmoto, B. Sutherland, and C. Tang, Phys. Rev. B **35**, 1020 (1987).
[24]J. Q. You, Q. B. Yand, and J. R. Yan, Phys. Rev. B **41**, 7491 (1990).
[25]H. Patel and D. Sherrington, Phys. Rev. B **40**, 11 185 (1989).
[26]J. A. Ashraff and R. B. Stinchcombe, Phys. Rev. B **39**, 2670 (1989).
[27]J. A. Ashraff, J-M. Luck, and R. B. Stinchcombe, Phys. Rev. B **41**, 4314 (1990).
[28]C. Benoit, J. Phys. C **20**, 765 (1987).
[29]C. Benoit, G. Poussigue, and A. Azougarh, J. Phys. Condens. Matter **2**, 2519 (1990); **1**, 335 (1989).
[30]The authors used the term "pseudo"-dispersion-curves to emphasize the singular continuous nature of the excitations.
[31]K. Niizeki and T. Akamatsu, J. Phys. Condens. Matter **2**, 2759 (1990).
[32]K. Niizeki, J. Phys. A **22**, 4295 (1989).
[33]E. E. Cherkashin, P. I. Kripyakevich, and G. I. Oleksiv, Kristallografiya **8**, 846 (1963) [Sov. Phys. Crystallogr. **8**, 681 (1964)].
[34]G. Bergman, J. T. Waugh, and L. Pauling, Acta Crystallogr. **10**, 154 (1957).
[35]C. A. Guryan, P. W. Stephens, A. I. Goldman, and F. W. Gayle, Phys. Rev. B **37**, 8495 (1988).
[36]V. Elser and C. L. Henley, Phys. Rev. Lett. **55**, 2883 (1985).
[37]M. Audier and P. Guyot, Philos. Mag. B **53**, L43 (1986).
[38]P. W. Stephens and A. I. Goldman, Phys. Rev. Lett. **56**, 1168 (1986).
[39]M. de Boissieu, C. Janot, J. M. Dubois, M. Audier, and B. Dubost, J. Phys. Condens. Matter **3**, 1 (1991).
[40]J. Los and T. Janssen, J. Phys. Condens. Matter **2**, 9553 (1990).
[41]T. Janssen (unpublished).
[42]F. W. Gayle, J. Mater. Res. **2**, 1 (1987).
[43]M. Audier, J. Pannetier, M. Leblanc, C. Janot, J. M. Lang,

and B. Dubost, Physica B **153**, 136 (1988).
[44]B. Dubost, J. M. Lang, M. Tanaka, P. Sainfort, and M. Audier, Nature (London) **324**, 48 (1986).
[45]M. J. Cooper and R. Nathans, Acta Crystallogr. **23**, 357 (1967).
[46]G. A. M. Reynolds, B. Golding, A. R. Kortan, and J. M. Parsey, Jr., Phys. Rev. B **41**, 194 (1990).
[47]M. deBoissieu, R. Currat, and C. Janot (unpublished).
[48]M. Audier and P. Guyot, in *Quasicrystals,* edited by M. V. Jaric and S. Lundqvist (World Scientific, Singapore, 1990), p. 74.
[49]A. I. Goldman, J. Shield, C. A. Guryan, and P. W. Stephens, in *Quasicrystals* (Ref. 48), p. 60.
[50]P. A. Bancel, Phys. Rev. Lett. **63**, 2741 (1989).
[51]C. L. Henley, in *Quasicrystals and Incommensurate Structures in Condensed Matter Physics,* edited by M. J. Yacaman, D. Romeu, V. Castano, and A. Gomez (World Scientific, Singapore, 1990), p. 152.
[52]M. Widom, in *Quasicrystals* (Ref. 48), p. 337.
[53]G. Coddens, R. Bellissent, Y. Calvayrac, and J. P. Ambroise (unpublished).
[54]For example, see C. Stassis, in *Methods of Experimental Physics,* edited by K. Skold and D. L. Price (Academic, San Diego, 1986), Vol. 23, pp. 369–441.
[55]See Ref. 1 for an explanation of various indexing schemes for icosahedral structures; also, see P. A. Bancel, P. A. Heiney, P. W. Stephens, A. I. Goldman, and P. M. Horn, Phys. Rev. Lett. **54**, 2422 (1985).
[56]The previously reported 15-meV excitation at the M_5 point, discussed in Ref. 5, could not be reproduced by the most recent experiments at the ILL.
[57]B. R. Doak (private communication).

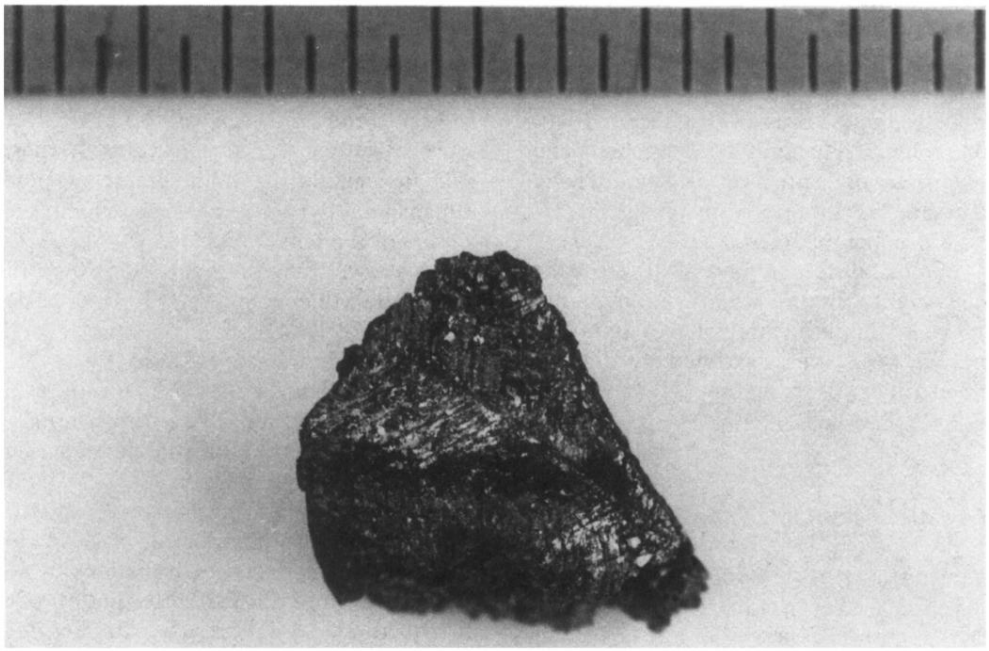

FIG. 3. Grain of icosahedral Al-Li-Cu used in the present measurements. The scale at the top is in millimeters.

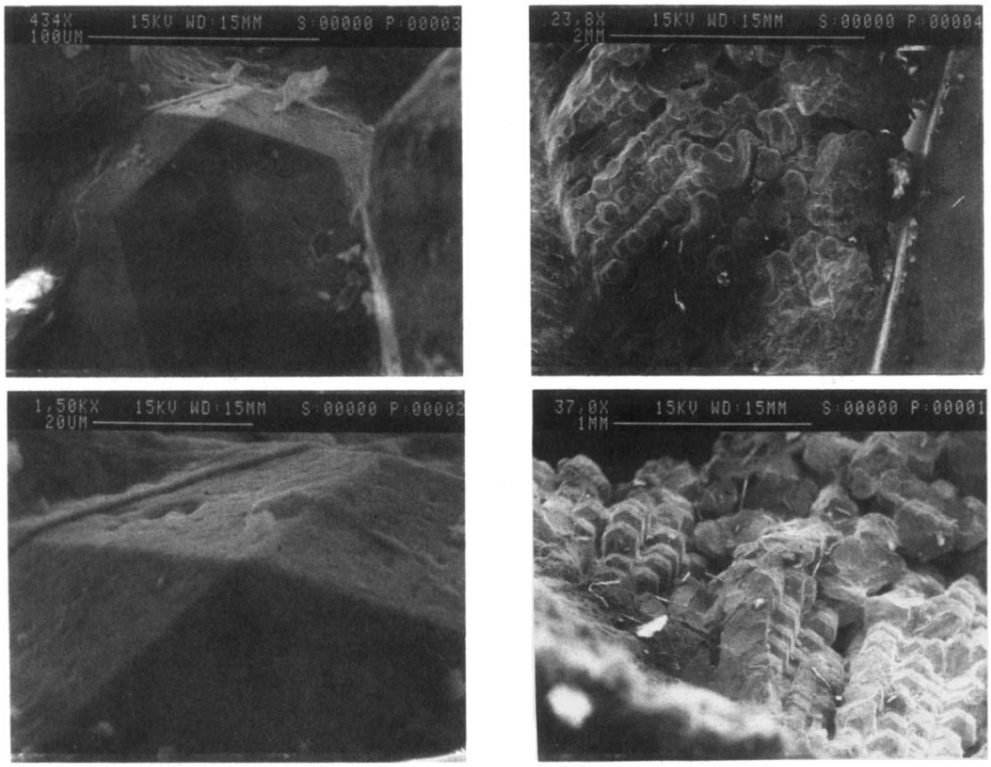

FIG. 4. Scanning-electron-microscope (SEM) photographs of the grain in Fig. 2, showing the microstructure of the surface. The scale of features is indicated in each photograph.